Title: Hierarchical control of microbial community assembly

Sammy Pontrelli[1], Rachel Szabo[2], Shaul Pollak[2], Julia Schwartzman[2], Daniela Ledezma-Tejeida[1], Otto X. Cordero[2], Uwe Sauer[1]

[1]Institute of Molecular Systems Biology, ETH Zürich, Switzerland
[2]Department of Civil and Environmental Engineering, Massachusetts Institute of Technology, Cambridge

One sentence summary: Specialized biopolymer degraders direct the trajectory of microbial community assembly through interconnected modes of nutrient crossfeeding.

Abstract:
Metabolic processes that fuel the growth of heterotrophic microbial communities are initiated by specialized biopolymer degraders that decompose complex forms of organic matter. It is unclear, however, to what extent degraders control the downstream assembly of the community that follows polymer breakdown. Investigating a model marine microbial community that degrades chitin, we show that chitinases secreted by different degraders produce oligomers of specific chain lengths that not only select for specialized consumers but also influence the metabolites secreted by these consumers into a shared resource pool. Each species participating in the breakdown cascade exhibits unique hierarchical preferences for substrates, which underlies the sequential colonization of metabolically distinct groups as resource availability changes over time. By identifying the metabolic underpinnings of microbial community assembly, we reveal a hierarchical crossfeeding structure that allows biopolymer degraders to shape the dynamics of community assembly.

Introduction

Microbial communities mediate a staggering number of biological processes that contribute to the health of humans, animals[1] and the planet as a whole[2]. The metabolic activity of co-occurring species results in the formation and depletion of nutrients in shared resource pools, where different modes of competition and cooperation impact community composition and form a network of metabolic crossfeeding[3,4,13–22,5,23,24,6–12]. Individual species often provide specific metabolic functions that influence the growth of a broader community, including use of terminal electron acceptors[14,25,26], degradation of complex carbon sources[27–30], removal of toxic byproducts[31–33], or assimilation of nitrogen and sulfur[18,34–36]. However, we remain with a limited molecular understanding of the extent to which individual species impact the formation and structure of crossfeeding networks and community assembly. Here, we demonstrate multiple metabolic mechanisms by which specialized biopolymer degraders influence the trajectory of community assembly, exemplified with an 18 member community that thrives on chitin, the second most abundant polysaccharide on the planet[37]. Similar to other polymer degrading communities[27–29], chitin communities require specialized degraders to supply nutrients to nonspecialized downstream consumers. Our community consists of phylogenetically diverse seawater isolates with distinct metabolic capabilities, which become abundant at different points during assembly of chitin communities. This provides a system that allows us to demonstrate how specialized chitin degraders initiate a hierarchal food web that shapes the community during the assembly process.

Functional classification of bacterial isolates

We first classified the 18 isolates, collected from natural polymer degrading communities[5,27](Table S1), into three functional guilds based on their phenotypic capabilities for chitin utilization (Fig 1A). These species were tested for the ability to grow on chitin, the chitin monomer *N*-acetylglucosamine (GlcNAc), and the dimer chitobiose (Fig 1AB, S1, S2): Five degraders used all three substrates as a sole carbon and

51 nitrogen source, and six exploiters could not use chitin but grew on GlcNAc, four of which also grew on
52 chitobiose. Seven scavengers could not use any of these substrates; hence, they must rely on nutrients
53 secreted by other species to thrive in the community. Previously published genome data of these 18
54 isolates[5,27] revealed a wide range of chitin utilization potential (Fig 1A) that closely matches phenotypes.
55 All five degraders, and two exploiters contain chitinases, uptake components specific for GlcNAc, and all
56 genes required for conversion of GlcNAc into glycolytic intermediates: GlcNAc kinase, GlcNAc-6-
57 phosphate deacetylase, and glucosamine-6-phosphate deaminase. The remaining four exploiters
58 contain all metabolic components required to metabolize and transport GlcNAc (Fig 1A). All seven
59 scavengers lack at least one transporter or catabolic gene required for GlcNAc utilization (Fig 1A). These
60 varying metabolic capabilities prime guilds to become abundant at different points during community
61 succession due to the different nutrients that become available over time[5]. To visualize the trajectory of
62 each functional guild during community assembly, we mapped 16s sequences of all species to 16s
63 ribosomal gene exact sequence variants whose abundance changes were previously determined on
64 chitin particles colonized from a large species pool in seawater[27]. The mean trajectories of each
65 functional guild revealed unique dynamics (Fig 1C), whereby degraders are the first to reach their
66 maximum abundance, followed by exploiters and finally scavengers. This succession pattern portrays an
67 order in a trophic cascade; i. e. degraders cause the release of chitin degradation products that are
68 consumed by exploiters, which in turn release broader sets of metabolites that support scavengers.
69

70 **Downstream metabolic influence of secreted chitinases**

71 It is likely that degraders form publicly available products that can support the growth of exploiters and
72 possibly select for specific species. To test this, extracellular enzymes were concentrated from culture
73 supernatants of each degrader during growth on chitin and used to digest fresh colloidal chitin. Liquid
74 chromatography mass spectrometry (LC-MS) quantification of oligosaccharides with six or fewer

75 residues revealed that each digest resulted in a unique oligomer profile, with the disaccharide
76 chitobiose and the monomer GlcNAc as the most abundant products (Fig 2A). Each of the six exploiters
77 was then grown on the five chitin digests (Fig 2B, Fig S3). *Sil*A3R06 and three other exploiters grew well
78 on all digests. While *Pha*B3M02 and *Alt*A3R04 hardly grew on the *Psy*6C06 digest that contained
79 chitobiose as the major oligomer (Fig 2A), but grew on *Vib*1A01 and *Psy*6C06 digests containing larger
80 quantities of GlcNAc and other oligomers (Fig 2A). Consistently, *Pha*B3M02 and *Alt*A3R04 did not grow
81 on chitobiose as the sole carbon source (Fig 2B, Fig S3). Inspired by this observation, we tested whether
82 the differences in hydrolysis product profiles among degraders could control which exploiters grow in
83 coculture. For this purpose, we grew degraders *Vib*1A01 and *Psy*6C06 in coculture with the four
84 exploiters. In accord with the enzyme digest data (Fig 2A), *Vib*1A01, which produces a range of
85 oligomers supported growth of all species in coculture (Fig 2D). The chitobiose producer *Psy*6C06 was
86 able to support all exploiters except *Pha*B3M02, showing that the composition of degradation products
87 can influence the abundance of specific exploiters. Surprisingly, the exploiter *Alt*A3R04 also grew in
88 coculture with *Psy*6C06, although it grew neither on the enzyme digest of *Psy*6C06 nor on chitobiose (Fig
89 2b). This suggests that additional metabolites were secreted by *Psy*6C06 or another exploiter to support
90 growth of *Alt*A3R04 but not of *Pha*B3M02, and more generally, that multiple resource pools are formed
91 during chitin degradation that allow downstream growth of less specialized species.
92
93 To understand the mechanism that facilitated the growth of AltA3R06 in coculture, we investigated
94 whether degraders secrete additional metabolites during growth on chitin to provide a carbon or
95 nitrogen source independent from GlcNAc oligomers. We grew the five degraders on colloidal chitin
96 until early stationary phase and inoculated the cell-free culture supernatants individually with six
97 exploiters and seven scavengers (Fig 2C). While four of the supernatants did not support growth of any
98 species to detectable optical densities, presumably because degraders consumed available limiting

99 nutrients required for growth, *Psy*6C06 supernatant supported the growth of six scavengers and three
100 exploiters. LC-MS targeted metabolomics revealed that GlcNAc and chitobiose concentrations were
101 below the limit of detection in all five supernatants. However, nine metabolites were present in at least
102 one supernatant, including succinate, glutamate, aspartate, and propionic acid (Fig S4, supplemental
103 dataset 1). Since catabolism of GlcNAc into the glycolytic intermediate glucose 6-phosphate entails
104 deacetylation and deamination, acetate or ammonia were quantified with enzyme assays (Fig 2E).
105 Ammonia was likely the nitrogen source provided to other species since it was present at substantial
106 concentrations in all supernatants. Acetate was present only in the *Psy*6C06 supernatant at a
107 concentration 10.9 fold higher than the cumulative molar concentrations of all other detected
108 metabolites. Hence, acetate was presumably the major carbon source in *Psy*6C06 cocultures that fueled
109 growth of *Alt*A3R04 (Fig 2D 2C). Collectively, these results demonstrate that non-degrading community
110 members are selectively supported by a combination of freely available chitin monomers, oligomers and
111 metabolic byproducts secreted during growth of degraders.
112
113 We suspected that exploiters also secrete metabolites that less specialized species consume, and
114 wondered if the chitin degradation products influence these secretion profiles. To test this hypothesis,
115 we cultivated each exploiter on colloidal chitin digested with extracellular enzymes obtained from each
116 of the five degraders. After 36 hours, culture supernatants were analyzed with the discovery
117 metabolomics method flow-injection time-of-flight (FIA-QTOF) MS[38]. Overall, we detected 2521 ions, of
118 which 216 could be annotated based on accurate mass. Principle component analysis using the 216
119 annotated ions showed a clear clustering of the secretion profiles based on the oligomer substrate (Fig
120 2F). For example, degraders *Vib*1A01 and *Vib*I3M07 produced similar sets of n1-n4 GlcNAc oligomers (Fig
121 2A). The secretion profiles of exploiters that used these substrates also showed no clear separation,
122 suggesting that *Vib*1A01 and *Vib*I3M07 exert similar effects on exploiters *via* their similar chitinases.

123 Alternatively, degraders *Psy*6C06 and *Vib*6D03 produced primarily chitobiose and GlcNAc, respectively,
124 and secretion profiles of exploiters grown on these digests clustered distinctly. These results
125 demonstrate that the different chitin degradation products play a major role in determining which
126 metabolites exploiters secrete into a shared resource pool.
127
128 **Identification of strain-specific metabolic secretion and uptake profiles**
129 We designed two experiments to identify which of the many secreted metabolites could potentially
130 serve as primary nutrient sources for scavengers. First, all scavengers were cultivated on cell-free
131 supernatants collected from each of the degraders and exploiters after growth on GlcNAc that was used
132 by all species. All supernatants except *Sil*A3R06 supported growth of at least two, but typically more
133 scavengers (5.27±2.4 with OD_{600} > 0.1, Fig 3A), demonstrating secretion of large quantities of
134 metabolites by most species. Measuring 24 absolute metabolite concentrations by targeted LC-MS and
135 enzymatic assays confirmed acetate and ammonia as the major carbon and nitrogen sources,
136 respectively (Fig 3BC, supplemental dataset 1), akin to the results obtained with the *Psy*6C06 chitin
137 supernatant. Yet, additional metabolic niches are manifested by a variety of organic acids, amino acids,
138 and nucleosides that made up as much 31% of the total secreted carbon pool, as in the case of
139 *Col*C2M11. The second experiment was designed to test how these additional metabolites are
140 partitioned among all community members. For this purpose, supernatants of degraders grown on
141 chitin and degraders and exploiters grown on GlcNAc were pooled into a single mixture containing all
142 secreted metabolites. All 18 strains were inoculated in this supernatant and grew individually to
143 densities between 0.15 and 0.7 OD_{600} units, corresponding to 4-6 doublings (Fig S5). To identify
144 consumed metabolites that support this growth, we determined relative changes by FIA-QTOF-MS and
145 searched for metabolites that were i) produced (log_2 fold change of ion intensity > 1) by degraders or
146 exploiters after growth to late exponential phase in at least one of the cultures, and ii) consumed (log_2 <

147 -0.5) by at least one species in samples taken over the course of growth in the pooled supernatant (Fig
148 3D, (Supplementary Dataset 2). Each species had a distinct metabolite consumption profile and a unique
149 ordered hierarchy of which metabolites are consumed first (Fig 3D). This was exemplified by acetate,
150 GlcNAc, pyruvate and glutamate (Fig 3E, Fig S6). For example, *Alt*A3R04 co-metabolized all four
151 substrates, while *Sil*A3R06 and *Pha*B3M02 metabolized them with specific ordered preferences or not at
152 all. These results suggest that species may be specialized to consume unique sets of resources with a
153 distinct hierarchy of preferences, thus enhancing the potential for many species to coexist in
154 environments with fluctuating nutrient availability.
155
156 Given the sequential colonization of degraders, exploiters, and scavengers (FIG 1C), we wanted to test
157 whether unique metabolic preferences of guilds and species drive this succession. For this purpose, we
158 approximated the availability of resource pools at early timepoints by determining which metabolites
159 are produced by degraders after individual growth on colloidal chitin, since chitin degradation initiates
160 community succession. Conversely, we approximated the resource pools that degraders and exploiters
161 produce at later timepoints by determining metabolites they secreted after growth on GlcNAc. We then
162 calculated the fraction of metabolites that each species consumed from the early or late resource pools
163 (Fig 3F). Of the 32 metabolites present in the chitin-derived resource pool, degraders, exploiters, and
164 scavengers consumed on average 13%, 28%, and 25% of the available metabolites, respectively.
165 Scavengers greatly increased their consumption to 45% of the 54 metabolites in the GlcNAc-derived
166 resource pool, while degrader and exploiter consumption did not change much. Thus, metabolites
167 produced at later timepoints in community succession are consumed preferentially by scavengers,
168 explaining how this functional guild is specialized to thrive on resources that become available at later
169 timepoints in community succession (Fig 1C).
170

171 **Metabolic interactions that define outcomes of chitin degrading communities**

172 In light of the unique secretion and uptake profiles of each species, we explored how these traits may
173 contribute to the outcome of communities in coculture. Cocultures were seeded with one of three
174 degraders and one of four exploiters with an additional set of the same four scavengers to create twelve
175 six-member communities (Fig 4A). The three degraders extracellularly produced different sets of chitin
176 degradation products (Fig 2A), which appeared to influence the prevalence of exploiters in several cases.
177 For example, exploiter *Alt*A3R04 used GlcNAc but not chitobiose (Fig 2B) and consistently coexisted well
178 with degrader *Vib*6D03 (Fig. 4A) that produced GlcNAc as a major degradation product (Fig 2A).
179 However, degrader-exploiter coexistence was not entirely explained by their dependence on GlcNAc
180 oligomers. For instance, exploiter *Col*C2M11 did not grow in coculture with degrader *Vib*1A01 (Fig. 4A),
181 despite its ability to grow on chitobiose and GlcNAc formed by *Vib*1A01(Fig 2A, S3). This is likely the
182 result of poor substrate affinity for GlcNAc oligomers and suggests that additional secreted metabolites
183 may fuel *Col*C2M11.

184

185 To gain a comprehensive view of metabolite exchange in cocultures, we compiled metabolite secretion
186 and uptake data of individual species (Supplementary Dataset 3) to construct 12 hypothetical nutrient
187 exchange networks with species combinations based on coculture outcomes observed in figure 4A.
188 Exchanged metabolites had the criteria of being liberated and/or secreted by a degrader during growth
189 on chitin and consumed by an exploiter or scavenger, or being secreted by an exploiter or scavenger and
190 consumed by a scavenger. Of 73 total metabolites included in these networks, each network on average
191 contained 29±8 metabolites and 65±27 exchanges thereof (Supplementary Dataset 4). No scavengers
192 coexisted with *Sil*A3R06 in any coculture (Fig 4A). To assess how exploiters influence the flow of
193 metabolites from degraders to scavengers, we identified potential competition for degrader-derived
194 metabolites by exploiters and scavengers from overlapping consumption profiles (Table S3). On average

195 *Sil*A3R06 consumes 80% of these degrader-derived metabolites, compared to at most 30% by any of the
196 other exploiters. To evaluate whether *Sil*A3R06 itself contributes metabolites to scavengers, we
197 calculated the percentage of metabolites produced by each exploiter that scavengers may consume
198 (Table S4), revealing that *Sil*A3R06 does not secrete any such metabolite. Thus, our hypothetical
199 networks suggest that *Sil*A3R06 likely competes with scavengers for available metabolites without
200 providing any growth-supporting substrates in return. Furthermore, these data illustrate how exploiters
201 have downstream influence on community diversity by changing the resources available to scavengers.
202
203 Beyond GlcNAc oligomers and other broadly secreted metabolites such as organic acids that may fuel
204 community succession (Fig 3B), we hypothesized that additional metabolites influenced the survival of
205 species in coculture. To this end, we used a Boolean modelling approach on the hypothetical networks
206 (Supplementary Dataset 4) to identify potential interactions that may explain the presence or absence of
207 species in coculture. We considered metabolites and strains as having only two possible states: present
208 or absent. By comparing metabolite and species state across the 12 networks, we determined which
209 metabolite exchanges were present only in conditions where the presence of a species was observed
210 (Table S2). Figure 4B illustrates the thus inferred flow of metabolites from degraders and exploiters to
211 scavengers in the investigated cocultures (Fig 4A). Among others (Table S2), primarily organic acids,
212 amino acids and one vitamin appear to contribute to community crossfeeding. In one example,
213 glutamate was predicted to feed the exploiter *Col*C2M11 from two degraders but not from *Vib*1A01 that
214 did not coexist with this exploiter, suggesting glutamate to be a growth-supporting metabolite for
215 *Col*C2M11. Also included in figure 4A are metabolites that were commonly produced by degraders and
216 exploiters (Fig 3B) which were shown to be consumed by scavengers (Fig 3D), such as glutamate,
217 pyruvate, oxoproline and the major growth supporting carbon source acetate (Fig 3B). Collectively,

218 these metabolite exchanges illustrate both the potential flow of metabolites that links functional guilds
219 as a whole (Fig 1A, 4B), and how specific metabolites contribute to the presence of individual species.
220
221 **Discussion**
222 Resolving microbial community function to the level of contributing species is hampered by the difficulty
223 in monitoring how nutrients are dispersed between species and how individual species can impact the
224 broader community through metabolic interaction networks. Here we demonstrate an approach for
225 how community interaction networks can be learned from the characterization of individual species,
226 and how specialized biopolymer degraders scaffold these networks to shape the population. Degraders
227 secrete chitinases that produce different oligomer profiles that influence the abundance of exploiters,
228 which thrive primarily on oligomers that they cannot generate themselves. Moreover, the composition
229 of oligomer profiles influences which metabolites exploiters secrete into a shared resource pool that is
230 available to the entire population. As such, degraders initiate a hierarchical cascade of nutrient flow into
231 a population.
232
233 An open question regarding the exchange of nutrients in a community is the extent to which it is
234 mediated by broad and nonspecific crossfeeding networks[6], or by species-specific interactions with an
235 ordered structure[7]. Our results provide evidence that the exchange of nutrients has an ordered
236 structure that allows individual species to shape the flow of metabolites, and subsequently that
237 nonspecific crossfeeding networks do not capture the complexity of nutrient exchange. We show that a
238 multitude of secreted metabolites provide metabolic niches to support a large population. However, our
239 results further demonstrate that scavengers, which can neither grow on chitin nor its degradation
240 products, preferentially consume metabolites that are formed at later points in community succession,
241 demonstrating how degraders scaffold downstream colonization of non-specialized species. With our

approach of integrating individual species consumption and secretion data, we were able to infer metabolic exchange networks that hypothesize specific metabolites that support growth of different species.

Collectively, these results demonstrate how a hierarchical structure is formed within microbial communities by radiating crossfeeding networks. In principle, this crossfeeding structure can be generalized to the multitude of communities that require specialized biopolymer degraders, including those involved in human health[1]and biogeochemical transformations[2]. Although hierarchical structures may be convoluted in more complex environments, we outline a concept for generating hypotheses on crossfeeding networks when constructing smaller consortia that recapitulate key aspect of the entire community.

References

1. Turnbaugh, P. J. *et al.* The Human Microbiome Project. *Nature* **449,** 804–810 (2007).
2. Konopka, A. What is microbial community ecology. *ISME J.* **3,** 1223–1230 (2009).
3. Ponomarova, O. *et al.* Yeast Creates a Niche for Symbiotic Lactic Acid Bacteria through Nitrogen Overflow. *Cell Syst.* **5,** 345–357.e6 (2017).
4. Baran, R. *et al.* Exometabolite niche partitioning among sympatric soil bacteria. *Nat. Commun.* **6,** (2015).
5. Datta, M. S., Sliwerska, E., Gore, J., Polz, M. F. & Cordero, O. X. Microbial interactions lead to rapid micro-scale successions on model marine particles. *Nat. Commun.* **7,** (2016).
6. Goldford, J. E. *et al.* Emergent simplicity in microbial community assembly. *Science (80-.).* **361,** 469–474 (2018).
7. Blasche, S. *et al.* Metabolic cooperation and spatiotemporal niche partitioning in a kefir microbial community. *Nat. Microbiol.* **6,** 196–208 (2021).
8. Pacheco, A. R., Moel, M. & Segrè, D. Costless metabolic secretions as drivers of interspecies interactions in microbial ecosystems. *Nat. Commun.* **10,** (2019).

273 9. Louca, S. *et al.* High taxonomic variability despite stable functional structure across microbial
274 communities. *Nat. Ecol. Evol.* **1,** 1–12 (2017).

275 10. Cordero, O. X., Ventouras, L. A., DeLong, E. F. & Polz, M. F. Public good dynamics drive evolution
276 of iron acquisition strategies in natural bacterioplankton populations. *Proc. Natl. Acad. Sci. U. S.*
277 *A.* **109,** 20059–20064 (2012).

278 11. Hehemann, J. H. *et al.* Adaptive radiation by waves of gene transfer leads to fine-scale resource
279 partitioning in marine microbes. *Nat. Commun.* **7,** (2016).

280 12. Romine, M. F., Rodionov, D. A., Maezato, Y., Osterman, A. L. & Nelson, W. C. Underlying
281 mechanisms for syntrophic metabolism of essential enzyme cofactors in microbial communities.
282 *Nat. Publ. Gr.* **11,** 1434–1446 (2017).

283 13. Kešnerová, L. *et al.* Disentangling metabolic functions of bacteria in the honey bee gut. *PLoS Biol.*
284 **15,** 1–28 (2017).

285 14. Stams, A. J. M. & Plugge, C. M. Electron transfer in syntrophic communities of anaerobic bacteria
286 and archaea. *Nat. Rev. Microbiol.* **7,** 568–577 (2009).

287 15. Wei, Z. *et al.* Trophic network architecture of root-associated bacterial communities determines
288 pathogen invasion and plant health. *Nat. Commun.* (2015). doi:10.1038/ncomms9413

289 16. Rodionov, D. A. *et al.* Micronutrient Requirements and Sharing Capabilities of the Human Gut
290 Microbiome. **10,** 1–22 (2019).

291 17. Moens, F., Verce, M. & De Vuyst, L. Lactate- and acetate-based cross-feeding interactions
292 between selected strains of lactobacilli, bifidobacteria and colon bacteria in the presence of
293 inulin-type fructans. *Int. J. Food Microbiol.* **241,** 225–236 (2017).

294 18. Gallon, J. R. N2 fixation in phototrophs: Adaptation to a specialized way of life. *Plant Soil* **230,** 39–
295 48 (2001).

296 19. Kramer, J., Özkaya, Ö. & Kümmerli, R. Bacterial siderophores in community and host interactions.
297 *Nat. Rev. Microbiol.* **18,** 152–163 (2020).

298 20. Zelezniak, A. *et al.* Metabolic dependencies drive species cooccurrence in diverse microbial
299 communities. *Proc. Natl. Acad. Sci. U. S. A.* **112,** E7156 (2015).

300 21. Venturelli, O. S. *et al.* Deciphering microbial interactions in synthetic human gut microbiome
301 communities. *Mol. Syst. Biol.* **14,** 1–19 (2018).

302 22. Weiss, A. S. *et al.* Exploring the interaction network of a synthetic gut bacterial community.
303 *bioRxiv* 2021.02.25.432904 (2021).

304 23. Bajic, D. & Sanchez, A. The ecology and evolution of microbial metabolic strategies. *Curr. Opin.*
305 *Biotechnol.* **62,** 123–128 (2020).

306 24. Cole, J. K. *et al.* Phototrophic biofilm assembly in microbial-mat-derived unicyanobacterial
307 consortia: Model systems for the study of autotroph-heterotroph interactions. *Front. Microbiol.*
308 **5,** 1–18 (2014).

309 25. Stams, A. J. M. *et al.* Exocellular electron transfer in anaerobic microbial communities. *Environ.*
310 *Microbiol.* **8,** 371–382 (2006).

311 26. Ha, P. T. *et al.* Syntrophic anaerobic photosynthesis via direct interspecies electron transfer. *Nat.*
312 *Commun.* **8,** 1–7 (2017).

313 27. Enke, T. N. *et al.* Modular Assembly of Polysaccharide-Degrading Marine Microbial Communities.
314 *Curr. Biol.* **29,** 1528–1535.e6 (2019).

315 28. Flint, H. J., Scott, K. P., Duncan, S. H., Louis, P. & Forano, E. Microbial degradation of complex
316 carbohydrates in the gut. *Gut Microbes* **3,** (2012).

317 29. Bayer, E. A., Morag, E. & Lamed, R. The cellulosome - a treasure- trove for biotechnology. **12,**
318 259–265 (1994).

319 30. Belzer, C. *et al.* Microbial Metabolic Networks at the Mucus Layer Lead to Diet-Independent
320 Butyrate and Vitamin B12 Production by Intestinal. *MBio* **8,** 1–14 (2017).

321 31. Bayer, B. *et al.* Proteomic Response of Three Marine Ammonia-Oxidizing Archaea to Hydrogen
322 Peroxide and Their Metabolic Interactions with a Heterotrophic Alphaproteobacterium. 1–15
323 (2019).

324 32. Morris, J. J., Johnson, Z. I., Szul, M. J., Keller, M. & Zinser, E. R. Dependence of the
325 cyanobacterium Prochlorococcus on hydrogen peroxide scavenging microbes for growth at the
326 ocean's surface. *PLoS One* **6,** (2011).

327 33. Lilja, E. E. & Johnson, D. R. Segregating metabolic processes into different microbial cells
328 accelerates the consumption of inhibitory substrates. *ISME J.* **10,** 1568–1578 (2016).

329 34. Kiene, R. P., Linn, L. J. & Bruton, J. A. New and important roles for DMSP in marine microbial
330 communities. **43,** 209–224 (2000).

331 35. Morono, Y. *et al.* Carbon and nitrogen assimilation in deep subsea fl oor microbial cells. **108,**
332 (2011).

333 36. Yesiltepe, Y. *et al.* Nitrogen Source Governs Community Carbon Metabolism in a Model
334 Hypersaline Benthic Phototrophic Biofil. *Msystems* 1–12 (2020).

335 37. Peter, M. G. Applications and Environmental Aspects of Chitin and Chitosan. *J. Macromol. Sci.*
336 *Part A* **32,** 629–640 (1995).

337 38. Fuhrer, T., Heer, D., Begemann, B. & Zamboni, N. High-throughput, accurate mass metabolome
338 profiling of cellular extracts by flow injection-time-of-flight mass spectrometry. *Anal. Chem.* **83,**
339 7074–7080 (2011).

340

Acknowledgments

Funding: This work was supported by a grant from the Simons Foundation (ID608247, SP and ID542395 OXC), as part of the collaboration on Principles of Microbial Ecosystems (PriME).

Author contributions: S Pontrelli designed and performed all experiments, analyzed data and wrote the manuscript. R Szabo performed genomic analysis of bacterial isolates. S Pollak mapped 16s sequences of bacterial isolates to ESVs of developing chitin communities. J Schwartzman performed 16s amplicon sequencing analysis. D Ledezma performed network analysis of chitin coculture outcomes. O Cordero assisted in data interpretation and writing the manuscript U Sauer designed the experiments and wrote the manuscript.

Competing interests: Authors declare no competing interests

Data availability: Metabolomics spectral files can be accessed from the MassIVE database and will be made publicly available upon publication. The short read 16 s rRNA amplicon sequencing data (BioSample: SAMN11023523-SAMN11023755) have been deposited in NCBI with the BioProject identifier PRJNA478695. All deposited genome sequences have been deposited in NCBI with BioProject identifier and BioSample IDs specified in table S1.

Supplementary datasets

Supplementary Dataset 1: LC-MS measurements of metabolites produced by degraders and exploiters after growth on chitin or GlcNAc

Supplementary Dataset 2: FIA-QTOF-MS measurements of metabolites produced by degraders and exploiters after growth on GlcNAc or chitin, measurements of metabolites produced by exploiters after growth on enzyme digest of degraders, and measurements of metabolites produced and consumed by all strains after growth on pooled supernatant

Supplementary Dataset 3: Compiled metabolite production and consumption data of each species that participated in 6 member chitin cocultures. This data was used for coculture specific metabolic network construction. The production and consumption data is compiled from individual metabolite production and consumption data of degraders grown on chitin, GlcNAc oligomers that degraders form extracellularly, secretion profiles of exploiters after growth in pooled supernatant, and metabolites consumed by exploiters and scavengers in pooled supernatant.

Supplementary Dataset 4: 12 Hypothetical metabolic exchanged networks that were constructed based on the outcome of six member chitin degrading cocultures.

Supplementary Dataset 5: Proteins related to chitin degradation and metabolism found to be present in the species used in this work.

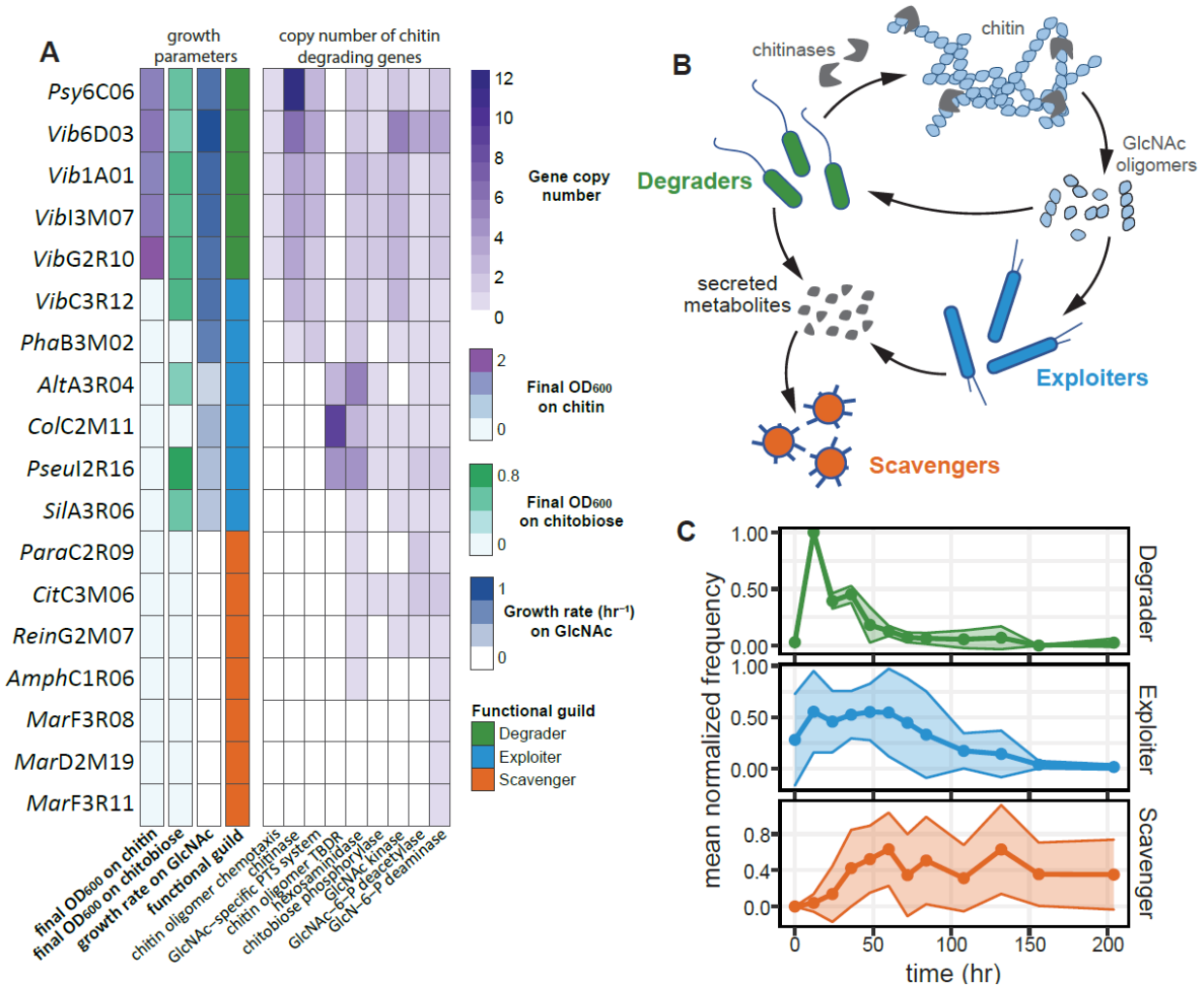

Figure 1: Successional dynamics of chitin degrading seawater communities. A) Species used in this study. Heatmap depicting (left to right) final OD_{600} after growth on 2 g/l colloidal chitin, final OD_{600} after growth on 10 mM chitobiose, growth rate on 20 mM GlcNAc, classified functional guild, and copy numbers of genes relevant for chitin degradation. Growth data was obtained from three independent biological replicates. B) Schematic of functional guilds: Degraders can grow on chitin as a sole carbon source through breakdown of chitin using chitin degrading enzymes, exploiters can grow on monomeric or oligomeric N-acetylglucosamine (GlcNAc) as a sole carbon source, and scavengers require metabolites secreted by other species to be sustained in the community. C) 16s sequences of the 18 investigated species are mapped to 16s ribosomal gene exact sequence variants whose abundances were previously determined on chitin particles colonized from a species pool in seawater[27]. Mean normalized frequencies of species that comprise each functional guild are plotted over time. TBDR, TolB-Dependent receptor

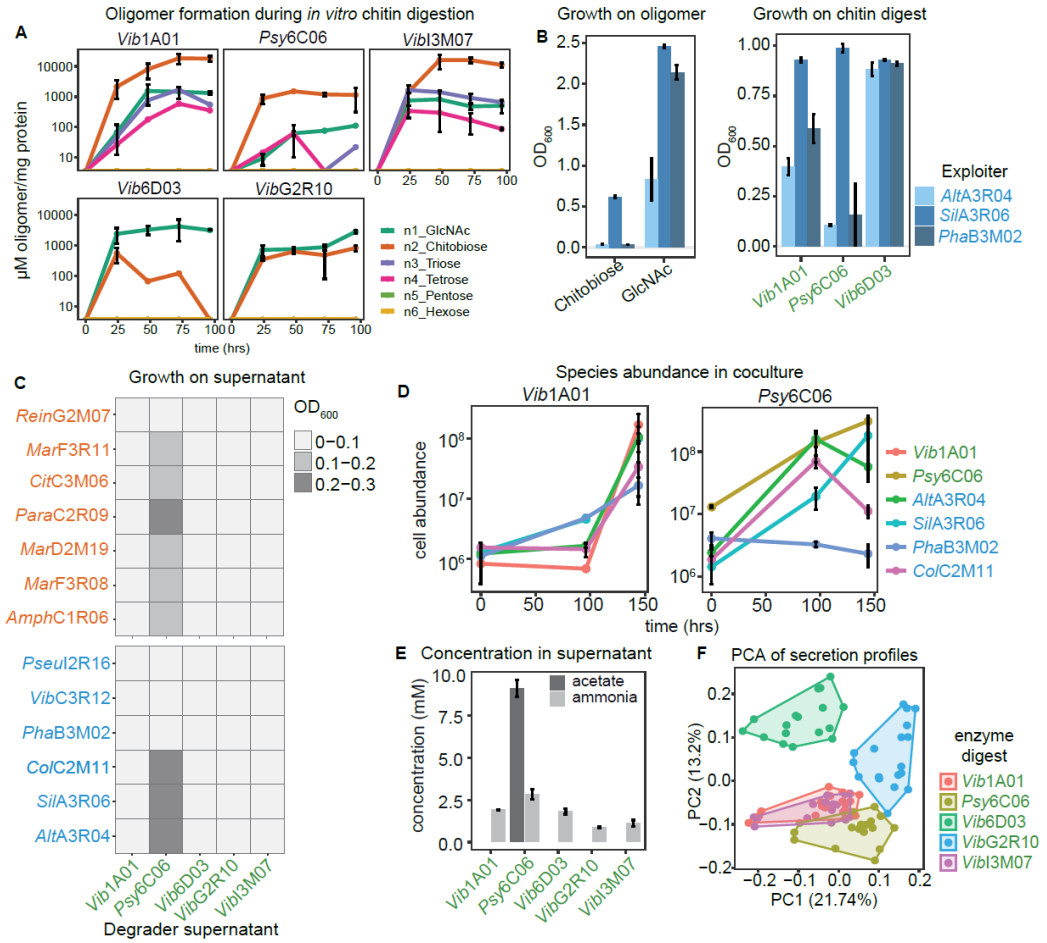

Figure 2: Chitin degradation products influence exploiter population and their secreted resources A) Quantification of GlcNAc oligonucleotide during *in vitro* digestion of 5 g/l chitin by secreted enzymes from each degrader. B) OD_{600} of three exploiters after 36 h growth on 20 mM GlcNAc, 10 mM chitobiose, and three enzyme digests. C) Growth of scavengers and exploiters after 36 hours on cell-free supernatant produced by each of the five degraders upon growth on colloidal chitin. D) Absolute abundance of species in cocultures of one degrader (*Vib*1A01 or *Psy*6C06) and four exploiters during grown on colloidal chitin, as determined by qPCR. E) Enzymatic quantification of ammonia and acetate in degrader supernatants upon growth on colloidal chitin. F) Principal component analysis exploiter metabolite secretion profiles after growth on each colloidal chitin digest. Colors represent the digest used as a growth substrate. All error bars represent standard deviation from three biological replicates.

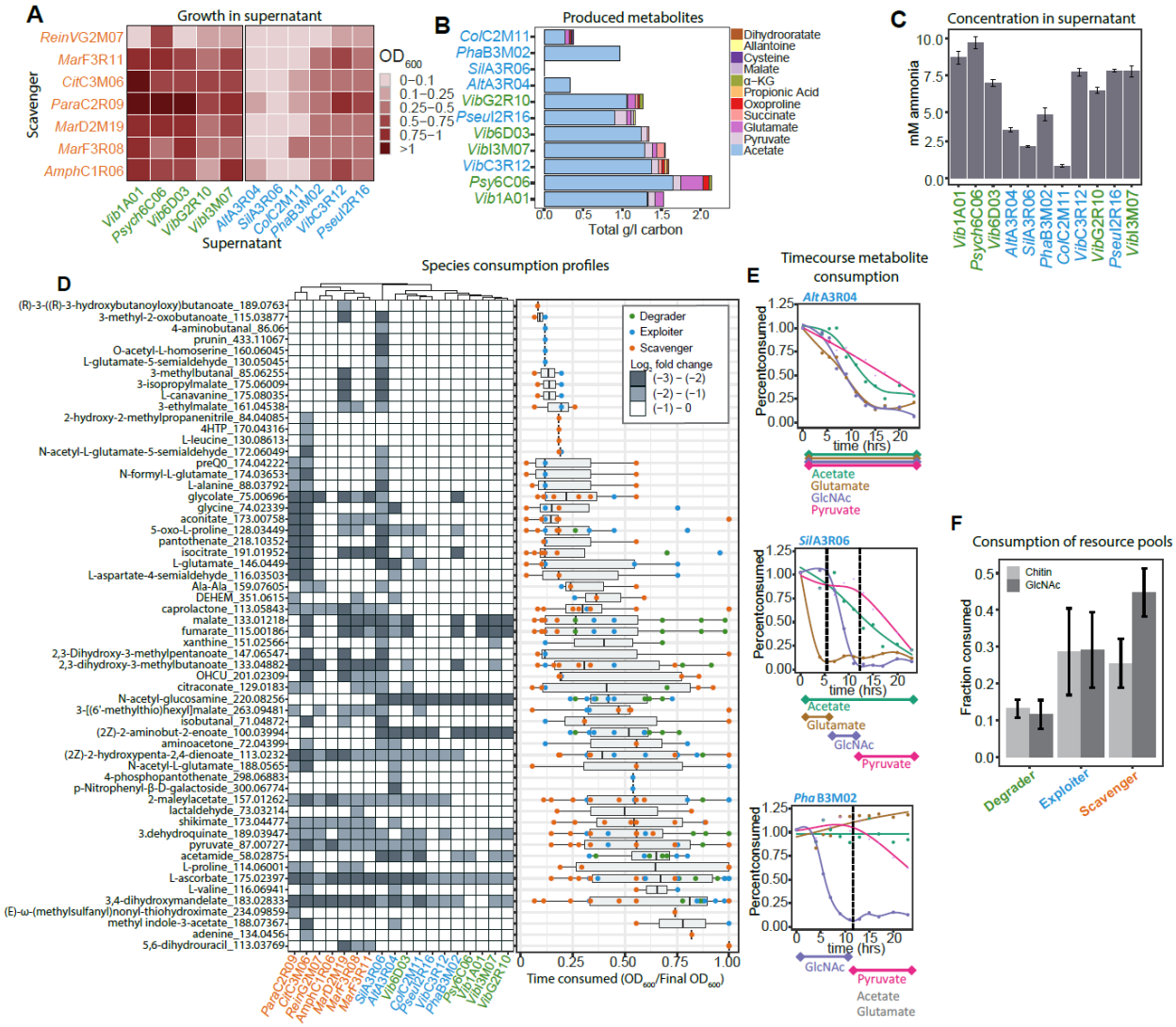

Figure 3: Metabolite consumption and production profiles among community members A) Growth of scavengers at 36 hours on cell-free supernatants obtained from degraders and exploiters after growth on GlcNAc. B) Metabolite concentration in cultures of degraders or exploiters after growth on 20 mM GlcNAc. C) Ammonia concentration in cultures of degraders or exploiters after growth on GlcNAc. D) Consumption of crossfed metabolites in pooled supernatant. (left) FIA-QTOF-MS measurements of metabolites that are consumed by degraders, exploiters or scavengers (Ion intensity $Log_2 < -0.5$). (right) Time course measurements of metabolite consumption. Points represent the fraction of the final OD_{600} at which metabolite consumption is detected for each species E) Relative change of acetate, pyruvate, GlcNAc, and glutamate during growth in pooled supernatant by three exploiters. Curves are fit using local polynomial regression. F) Fraction of available metabolites contained in chitin or GlcNAc derived resource pools that is consumed by each functional guild. All experiments were performed in triplicate. Error bars represent standard deviation. DEHEM, 4-deoxy-α-L-erythro-hex-4-enopyranuronate-β-D-mannuronate; OHCU, 2-oxo-4-hydroxy-4-carboxy-5-ureidoimidazoline. Strain names in green are degraders, blue are exploiters, and orange are scavengers.

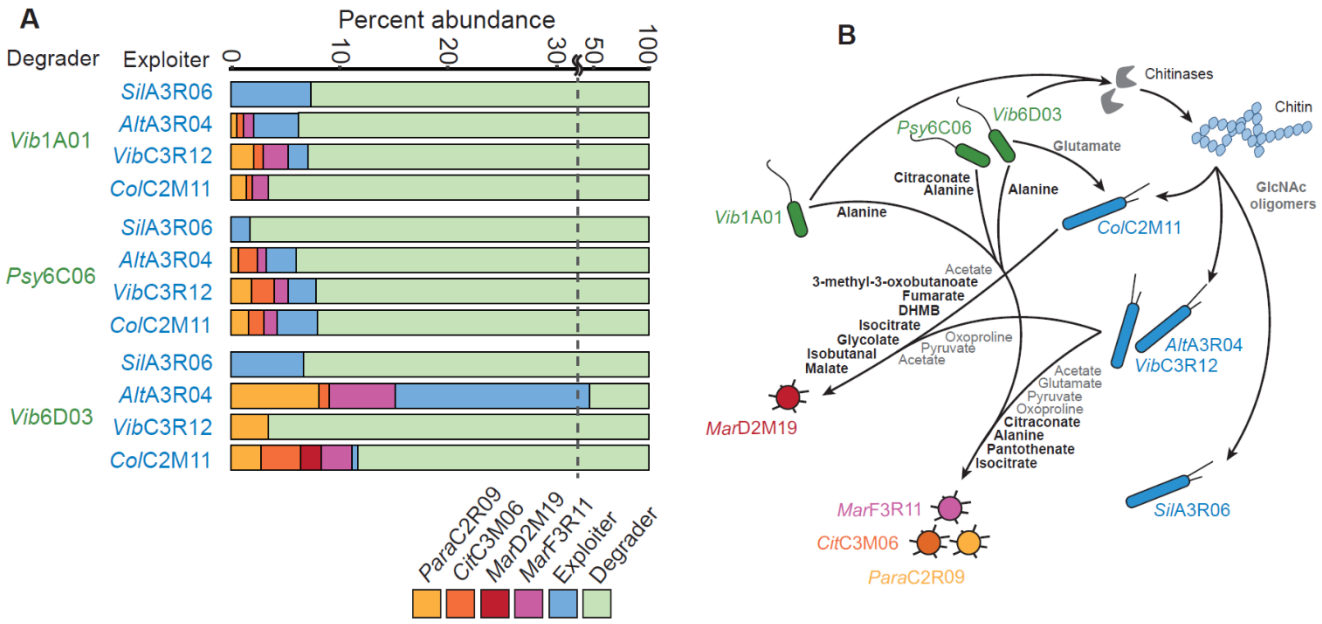

Figure 4: Outcomes of chitin degrading cocultures and underlying metabolic crossfeeding network A) Each coculture was seeded with six species: one degrader (green), one exploiter (blue), and each of the four scavengers *Para*C2R09 (yellow), *Cit*C3M06 (orange), *Mar*D2M19 (red), *Mar*F3R11 (purple). Cultures were grown for five weeks with four serial dilutions on colloidal chitin and relative abundance is shown for the final culture. Experiments were performed in triplicate. B) Network illustration of metabolites that fuel species growth in the cocultures of panel A. Metabolites commonly secreted by degraders or exploiters and known to be consumed by scavengers are shown in grey. All bolded metabolites were identified using a Boolean modelling approach from the coculture outcomes in panel A. All remaining secreted metabolites and crossfeeding interactions that are not represented in this illustration are contained in (Supplementary Dataset 1, Supplementary Dataset 4). Abbreviation: DHMB, 2,3-dihydroxy-2-methylbutanoate